Neisseria gonorrheae O-Acetylpeptidoglycan Esterase, a Serine Esterase with a Ser-His-Asp Catalytic Triad†

Joel T. Weadge‡ and Anthony J. Clarke*

Department of Molecular and Cellular Biology, University of Guelph, Guelph, Ontario N1G 2W1, Canada

Received February 6, 2007; Revised Manuscript Received February 22, 2007

ABSTRACT: *O*-Acetylpeptidoglycan esterase from *Neisseria gonorrheae* FA1090 is similar in sequence to family CE-3 carbohydrate esterases of the CAZy classification system, and it functions to release O-linked acetyl groups from the C-6 position of muramoyl residues in O-acetylated peptidoglycan. Here, we characterize the peptidoglycan of *N. gonorrheae* FA1090 as being O-acetylated and find that it serves as a substrate for the esterase. The influence of pH on the activity of *O*-acetylpeptidoglycan esterase was determined, and pK_a values of 6.38 and 6.78 for the enzyme−substrate complex (VE_t^{-1}) and free enzyme ($VE_t^{-1}K_M^{-1}$), respectively, were calculated. The enzyme was inactivated by sulfonyl fluorides but not by EDTA. Multiple-sequence alignment of the *O*-acetylpeptidoglycan esterase family 1 enzymes with members of the CE-3 enzymes and protein modeling studies identified Ser80, Asp366, and His369 as three invariant amino acid residues that could potentially serve as a catalytic triad. Replacement of each with alanine was accomplished by site-directed mutagenesis, and the resulting mutant proteins were purified to apparent homogeneity. The specific activity of each of the three esterase derivatives was greatly reduced on *O*-acetylpeptidoglycan. Using the artificial substrate *p*-nitrophenyl acetate, a kinetic analysis revealed that the turnover number (VE_t^{-1}) but not K_M was affected by the replacements. These data thus indicate that *N. gonorrheae O*-acetylpeptidoglycan esterase, and by analogy the CE-3 family of enzymes, function as serine esterases involving a Ser-His-Asp catalytic triad.

Peptidoglycan (PG)[1] is a unique heteropolymer found within the cell wall of most eubacteria. It is important to the bacteria because it provides shape and structural rigidity and resists the forces of turgor pressure for the cell. The repeating unit of PG is composed of two alternating sugars, *N*-acetylglucosamine linked β-1,4 to *N*-acetylmuramic acid (MurNAc) with a peptide side chain of L and D amino acids linked to the C-3 lactyl moiety of the latter amino sugar (Figure 1). An increasing number of bacteria have been identified with a further modification, an O-acetylation, to the C-6 hydroxyl of MurNAc (reviewed in refs *1* and *2*). In bacterial species known to O-acetylate their PG, no strain has been found to be either completely devoid of the modification or fully acetylated. The presence of this modification to PG is significant because it hinders sterically the activity of host defensive muramidases, such as the lysozymes, and totally precludes the function of the lytic transglycosylases, enzymes essential to the bacteria for the biosynthesis of PG (reviewed in refs *1* and *2*).

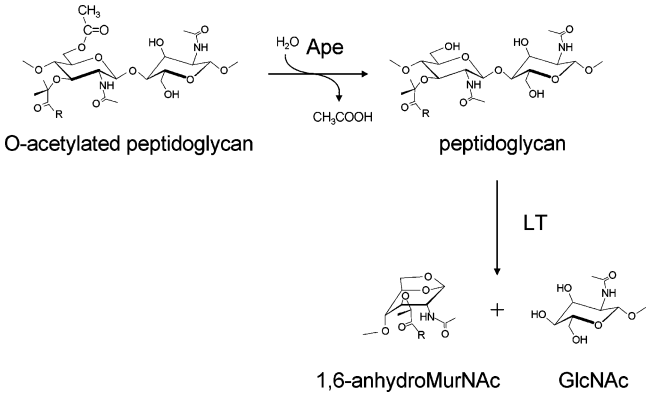

FIGURE 1: Structure of O-acetylated PG and functions of *O*-acetylPG esterase (Ape) and lytic transglycosylase (LT). PG is composed of alternating MurNAc and GlcNAc residues, and O-acetylation occurs on the C-6 hydroxyl group of the former to generate *N*,*O*-diacetylmuramoyl residues (N,O-diAcMur). Ape catalyzes the hydrolysis of O-acetyl groups, thereby renduring the PG product available for cleavage by LTs, which require a free C-6 hydroxyl group to generate their 1,6-anhydroMurNAc product. R denotes the stem muropeptide.

We recently discovered a new class of bacterial esterases encoded in the genomes of a number of bacteria, both Gram-positive and Gram-negative, that function to remove the acetate from the C-6 position of muramoyl residues in PG (Figure 1). Some of these bacteria, such as *Campylobacter jejuni*, *Helicobacter pylori*, *Neisseria gonorrheae*, and *Bacillus anthracis*, represent major human pathogens. Sequence alignment studies allowed us to arrange these *O*-acetylpeptidoglycan esterases (Apes) into families, with family 1 being

† This work was supported by an operating grant (MOP 81223) to A.J.C. from the Canadian Institutes of Health Research and a postgraduate scholarship (PGSB) to J.T.W. from the Natural Sciences and Engineering Research Council of Canada.

* To whom correspondence should be addressed. E-mail: aclarke@uoguelph.ca. Telephone: (519) 824-4120. Fax: (519) 837-1802.

‡ Present address: Carlsberg Laboratorium, Department of Chemistry, Gamle Carlsberg Vej 10, Valby, DK 2500 Denmark.

[1] Abbreviations: PG, peptidoglycan; MurNAc, *N*-acetylmuramic acid; Ape, *O*-acetylpeptidoglycan esterase; Axe, acetyl xylan esterase; *p*NP-acetate, *p*-nitrophenyl acetate; MSF, methanesulfonyl fluoride; PMSF, phenylmethanesulfonyl fluoride.

10.1021/bi700254m CCC: $37.00
Published on Web 03/28/2007

Table 1: Purification of Ape1a and Its Mutant Derivatives

enzyme	total protein (mg)	total activity[a] (μmol/min)	specific activity[b] (μmol min^{-1} mg^{-1})	purification (x-fold)	yield (%)
Ape1a					
cell lysate	567	103	0.182	1	100
Ni^{2+}NTA-agarose	13.6	40.1	2.96	16.3	38.9
Source S	2.56	21.9	8.54	46.9	21.2
Asp366 → Ala					
cell lysate	495	15.3	0.0309	1	100
Ni^{2+}NTA-agarose	11.2	5.08	0.453	14.7	7.91
Source S	1.2	1.68	1.4	45.3	7.35
His369 → Ala					
cell lysate	964	23	0.0238	1	100
Ni^{2+}NTA-agarose	19.5	0.962	0.0494	2.07	4.18
Source S	4.52	0.532	0.118	4.93	2.31
Ser80 → Ala					
cell lysate	562	10.4	0.0185	1	100
Ni^{2+}NTA-agarose	17.2	0.672	0.0392	2.12	6.46
Source S	4.37	0.396	0.0905	4.9	3.9

[a] Purification from 1 L cultures of respective *E. coli* transformants expressing the enzyme derivative. [b] Activity assayed using 2 mM *p*NP-acetate substrate in 50 mM sodium phosphate buffer at pH 7.0 and 25 °C.

further subdivided into three subfamilies (*3*). From these protein alignments, it was determined that members of the Ape1 family have sequences significantly similar to those of the family 3 carbohydrate esterases (CE-3) of the CAZy classification system which is comprised of acetyl xylan esterases. We subsequently cloned and expressed the *ape1a* gene from *N. gonorrheae* in *Escherichia coli*. Comparing Ape1a's k_{cat} for *p*-nitrophenyl acetate (*p*-NP-acetate) with the pseudo-first-order rate constant for the spontaneous hydrolysis of this synthetic substrate at the same temperature and pH, its catalytic power of 10^8-fold is similar to that of acetyl xylan esterases. However, in addition to acetyl xylan esterase activity, enzymatic studies confirmed that Ape1a had greater specificity for O-acetylated PG substrates (*4*). This latter characteristic is unique to this enzyme as previous studies by others have determined that authentic acetyl xylan esterases do not act on PG (*5*, *6*).

Given its apparent essential function in removing O-acetyl groups from PG thereby permitting the uninterrupted action of the lytic transglycosylases, we have proposed that Ape1 may serve as an attractive target for the development of a new class of antibacterial compounds (*4*). To explore this possibility, an understanding of its structure−function relationship is essential. No catalytic mechanism has yet been defined for the CAZy family CE-3 esterases. However, structural and mechanistic studies conducted on a PG *N*-acetylmuramic acid deacetylase from *Bacillus subtilis* (*7*), the *Streptococcus pneumoniae* PG *N*-acetylglucosamine acetylesterase (*8*), acetyl xylan esterases from *Clostridium thermocellum* (*9*) and *Streptomyces lividans* (*9*, *10*), and a chitin deacetylase from *Colletotrichum lindemuthianum* (*11*) indicate that each of these family CE-4 deacetylases functions as a metalloenzyme using a His-His-Asp zinc-binding triad with proximal aspartyl and histidyl residues acting as the catalytic base and acid. On the other hand, all other known acetyl xylan esterase structures exhibit an α/β-hydrolase fold and appear to involve a Ser-His-Asp catalytic triad (reviewed in ref *12*). Thus, it is believed that these latter enzymes, belonging to families CE-1, -5, -6, and -7, function as typical serine esterases with a Ser residue acting as the catalytic nucleophile for hydrolysis, but detailed mechanistic studies have not been conducted.

Alignment of the known and hypothetical amino acid sequences of the Ape1 and CE-3 esterases led to the identification of a number of invariant residues, including potential residues that may participate in the catalytic mechanism of the respective enzymes (*3*). In this study, we have used kinetic, inhibition, and protein engineering approaches to delineate the mechanism of action of *N. gonorrheae* Ape1a, and by analogy the CE-3 enzymes, as serine esterases.

EXPERIMENTAL PROCEDURES

Bacterial Strains and Growth Media. The sources of bacterial strains used, together with their genotypic description, are listed in Table 1 of the Supporting Information. *N. gonorrheae* strains FA1090 and 1291 were used for PG isolation and were maintained on GC medium base supplemented with Kellogg's defined supplement (*13*, *14*) in a humid, 5% CO_2 environment at 35 °C. *E. coli* DH5α was maintained on LB broth or agar at 37 °C. *E. coli* BL21-λDE3(pLysS), used for protein expression, was maintained on LB agar containing 35 μg/mL chloramphenicol. For the expression of high levels of proteins, *E. coli* BL21-λDE3 was always freshly transformed with plasmid constructs and was grown in Super Broth (5 g of sodium chloride, 20 g of yeast extract, and 32 g of tryptone) at 37 °C with agitation.

Chemicals and Reagents. Fisher Scientific (Nepean, ON) provided acrylamide, glycerol, pyridine, and Luria-Bertani (LB) growth medium, while DNase I, RNase A, Pronase, IPTG, and EDTA-free protease inhibitor tablets were purchased from Roche Molecular Biochemicals (Laval, QC). Mono S 5/5 was purchased from Amersham Pharmacia Biotech (Uppsala, Sweden), and Ni^{2+}NTA-agarose was a product of Qiagen (Valencia, CA). T_4 DNA ligase and restriction enzymes were from New England Biolabs (Mississauga, ON), while *pfu* turbo DNA polymerase and restriction endonuclease *Dpn*I were purchased from Stratagene (La Jolla, CA). All other chemicals and reagents were from Sigma Chemical Co. (St. Louis, MO).

To obtain appropriate yields, *O*-acetylPG was prepared from lawns of *N. gonorrheae* strains grown on at least 15 agar plates. Cells from these plates were scraped off and pooled in a minimal volume of 50 mM sodium phosphate

buffer (pH 6.0) at 4 °C. The insoluble PG from the cell suspensions was isolated as previously described by Dupont and Clarke (*15*) with care being taken to maintain the pH below 7.0 throughout the procedure to prevent unwanted base hydrolysis of the ester-linked acetate. Purification of the *O*-acetylPG from contaminating carbohydrates, nucleic acids, and proteins was achieved by digestion with α-amylase, DNase I, RNase A, and heat-treated Pronase as previously described (*15*).

Quantification of PG O-Acetylation. The release of ester-linked acetate from PG was achieved by incubating samples in 1 M NaOH for 2 h at room temperature. The insoluble, base-treated PG was subjected to centrifugation (5000*g* for 15 min), and the pellets were analyzed for muramic acid or protein content following their hydrolysis in 4 or 6 M HCl, respectively, at 105 °C for 18 h, in vacuo (*16*). The supernatants were analyzed for liberated acetate by two methods. The first involved HPLC-based organic acid analysis using an Aminex HPX-87H Bio-Rad column as previously described (*17*). For the second, we employed a coupled enzymatic assay (acetate kinase, phosphotransacetylase, pyruvate kinase, and lactate dehydrogenase) using the commercially available acetic acid kit (Megazyme International Ireland Ltd., Wicklow, Ireland) according to the manufacturer's specifications.

Production and Purification of Ape1a. The production and purification of the truncated, soluble derivative form of Ape1a (previously named ΔApe1a) used throughout these studies were as described previously (*4*) except for the method of protein isolation. Briefly, *E. coli* BL21-λDE3-(pLysS) cells were transformed with the appropriate plasmid construct. These cells were grown in SuperBroth at 37 °C to an OD_{600} of 0.6 and then induced with 1 mM IPTG (final concentration) for 3 h at 18 °C. Cells were isolated by centrifugation (5000*g* for 15 min at 4 °C) and stored at −20 °C until they were needed.

To purify the His_6-tagged proteins, cell pellets were thawed and resuspended in a minimal volume of lysis buffer [50 mM sodium phosphate (pH 8) and 500 mM sodium chloride]. Lysozyme (1 mg/mL), RNase A (10 μg/mL), and DNase I (5 μg/mL) were added to aid lysis, and in some cases, ethylenediaminetetraacetic acid (EDTA) free protease inhibitor tablets (1 per 15 mL of suspension) were added to prevent undesired protein degradation. The suspension was incubated at 4 °C for 30 min before being subjected to lysis in a French pressure cell (two passes at 18 000 psi). Unlysed cells were removed by centrifugation (5000*g* for 15 min at 4 °C), and 1 mL of Ni^{2+}NTA-agarose was added for every 15 mL of cleared lysate. The mixtures were incubated for 1 h at 4 °C with shaking before being applied to 15 mL disposable plastic columns. Unbound proteins were eluted, and the matrix was washed with approximately 10 column volumes of lysis buffer. The matrix was further washed with approximately 10 column volumes of wash buffer containing 20 mM imidazole and then 10 column volumes of wash buffer containing 30 mM imidazole. Bound proteins were recovered by batch elution in 10 mL of wash buffer containing 100 mM imidazole. The eluted protein mixtures were dialyzed for 16 h against 2 × 4 L of 25 mM sodium phosphate buffer (pH 7).

The His_6-tagged proteins were further purified by cation-exchange chromatography on Mono S. The protein was applied to the column following its equilibration in running buffer [25 mM sodium phosphate buffer (pH 7.0)] at a flow rate of 1 mL/min. Elution of the protein from the column was accomplished by increasing the ionic strength of the running buffer using a linear 0 to 1 M NaCl gradient. The His_6-tagged proteins were found to elute in buffer containing approximately 75 mM NaCl.

Enzyme Assays. For routine detection of acetyl esterase activity, 2 mM *p*NP-acetate in 50 mM sodium phosphate buffer (pH 6.5) was used as a substrate in a 96-well microtiter plate assay (*4*). Reactions involving a total volume of 300 μL were initiated by the addition of the *p*NP-acetate and were allowed to proceed for at least 5 min. The progress of reactions was monitored at 405 nm for the appearance of *p*-nitrophenol, and 1 unit of esterase activity was defined as the amount of enzyme required to release 1 μmol of *p*-nitrophenol min^{-1} (mg of protein)$^{-1}$.

The specificity of His_6-tagged Ape1 and its mutant derivatives for *N. gonorrheae O*-acetylPG was tested using an evenly dispersed 5 mg/mL suspension of insoluble PG (by sonication for 1 min) in 50 mM sodium phosphate buffer (pH 7.0). Triton X-100 was added to a final concentration of 0.1%, and reactions were initiated via the addition of enzyme. Reaction mixtures, performed in triplicate, were incubated at 37 °C and then reactions terminated by acidifying the reaction mixtures with 1 M H_2SO_4. Samples of substrate incubated in the absence of added enzyme served as controls for the spontaneous release of any acetate. Insoluble material was removed from the mixtures by centrifugation (5000*g* for 15 min) prior to analysis for liberated acetate as described above. One unit of activity is defined as the amount of enzyme required to produce 1 μmol of product in 1 min, and specific activities are reported as the average of at least three independent trials.

Effect of pH on Kinetic Parameters. The effect of pH on the Michaelis−Menten parameters of Ape1a was determined using *p*NP-acetate as a substrate by two different methods. In the first method, the hydrolysis of *p*NP-acetate was monitored as described above using substrate concentrations of 0.5−4.5 mM in 50 mM sodium acetate buffer (pH 3−6) and 50 mM sodium phosphate buffer (pH 5.5−8). Standard curves of *p*-nitrophenol at each pH that was tested were generated to normalize the effect of pH on the absorbance of *p*-nitrophenol, and no "product" inhibition was observed with the use of the acetate buffer. The second method monitored the production of *p*-nitrophenol using a discontinuous assay. Briefly, Ape1a was added to appropriate concentrations of substrate in 25 mM sodium acetate buffer (pH 3−6) and 25 mM sodium phosphate buffer (pH 5.5−8) and incubated at 30 °C. At specific time intervals, reactions were stopped with the addition of 1% SDS (final concentration) and the pH of the reaction mixture was adjusted to 7 by the addition of 0.5 M sodium phosphate. The production of *p*-nitrophenol at each time point could then be determined by measuring the absorbance at 405 nm. For both methods, each analysis was performed in triplicate and plots of initial reaction velocities as a function of substrate concentration were analyzed by nonlinear regression using Microcal Origin 6.0 assuming a one-site binding model. The pK_a values of the free enzyme and enzyme−substrate complex were also determined in the same fashion by plotting $VE_t^{-1}K_M^{-1}$ versus

Table 2: Kinetic Parameters of Ape1a and Its Mutant Derivatives[a]

	K_M (mM)	V/E_t (s^{-1})	VE_tK_M (M^{-1} s^{-1})
Ape1a	0.51 ± 0.21	10.1 ± 4.1	2.0×10^4 (100%)[b]
D366A Ape1a	0.70 ± 0.49	0.813 ± 0.57	1.2×10^3 (6.0%)[b]
H369A Ape1a	1.1 ± 0.51	0.332 ± 0.15	3.0×10^2 (1.5%)[b]
S80A Ape1a	0.97 ± 0.61	0.00029 ± 0.00023	2.9×10^{-1} (0.0014%)[b]

[a] Reactions were conducted (in triplicate) in 50 mM sodium phosphate buffer at pH 6.5 and 20 °C. [b] Percentages in parentheses were calculated relative to Ape1a.

the H^+ concentration and V/E_t versus the H^+ concentration, respectively.

Inhibition Studies. The inhibitory effect of different reagents was tested in 50 mM sodium phosphate buffer (pH 6.5) containing 375 μg of Ape1a in a microtiter plate assay. Methanesulfonyl fluoride (MSF) dissolved in 2-propanol and phenylmethanesulfonyl fluoride (PMSF) dissolved in ethanol were tested at various concentrations over specific periods of time, and then the specific activity of the treated enzyme preparations was assayed directly by the addition of substrate (2.5 mM *p*NP-acetate). Metal ions (Mg^{2+}, Ca^{2+}, Mn^{2+}, and Zn^{2+}) as their chloride salts and EDTA were all tested at concentrations of 1 mM. Each was incubated with the enzyme for 30 min at 30 °C before being assayed for residual activity. Values are reported as the percent residual activity relative to the untreated enzyme controls, and IC_{50} values were determined.

Site-Directed Mutagenesis of ape1a. Asp366, His369, and three Ser residues, Ser80, Ser152, and Ser308, in Ape1a were replaced with Ala by site-directed mutagenesis of the *ape1* gene. Primers used for this mutagenesis are listed in Table 2 of the Supporting Information. Mutagenesis was carried out using pACJW16 (for Δ*ape1a*) as a template for *pfu* Turbo DNA polymerase according to the QuickChange site-directed mutagenesis kit (Stratagene, La Jolla, CA). Following PCR, 1 mL of *Dpn*I was added to a 50 μL PCR mixture and incubated for at least 1 h at 37 °C to remove the original, methylated template. The resulting plasmids were used to transform *E. coli* DH5α, and clones were screened for the correct mutations by DNA sequencing. Each of the protein products was purified to apparent homogeneity as described above for wild-type Ape1a. Care was taken to use new (i.e., unused) chromatography media for each purification to preclude potential contamination of the various mutant forms of the enzymes with each other.

Structural Studies by Circular Dichroism Spectrometry. Spectra were collected using a Jasco (Tokyo, Japan) J-810 spectrapolarimeter. Far-UV spectra were recorded in a 0.1 cm path length cell while an internal temperature of 25 °C was maintained with a Julabo (Allentown, PA) F25ME heating water bath. An average of four accumulations was used to generate spectra, with a scan speed of 50 nm/min, a bandwidth of 1 nm, a data pitch of 0.2 nm, and a range of 260−180 nm. Further analysis of the spectra was performed with DICHROWEB (http://www.cryst.bbk.ac.uk/cdweb/html/home.html) using the Selecon 3 program with protein reference set 3 (*18*, *19*).

Enzyme Kinetic Studies. The Michaelis−Menten parameters of Ape1 and its mutagenic derivatives were determined using *p*NP-acetate as a substrate at concentrations of 0.05−4.5 mM. Each analysis was performed in triplicate, and plots of initial reaction velocities as a function of substrate concentration were analyzed by nonlinear regression using Microcal Origin 6.0 assuming a one-site binding model (*4*).

Other Analytical Techniques. Protein concentrations were determined by either amino acid analysis using a Beckman System Gold amino acid analyzer (Beckman Coulter Canada Inc., Mississauga, ON) following the hydrolysis of samples in 6 M HCl at 105 °C for 24 h in vacuo or the bicinchoninic acid assay (Pierce, Rockford, IL). SDS−PAGE was performed by the method of Laemmeli (*20*) using 12% acrylamide gels and staining with Coomassie Brilliant Blue. Sequence alignments were conducted using ClustalW version 1.8 (http://www.ebi.ac.uk/clustalw) followed by manual adjustments, while secondary structure predictions were performed using Jpred (http://www.compbio.dundee.ac.uk/~www-jpred/). Three-dimensional modeling of Ape1a was performed using both Phyre (http://www.sbg.bio.ic.ac.uk/~phyre/) and 3D-PSSM (http://www.sbg.bio.ic.ac.uk/~3dpssm/index2.html) (*21*−*23*).

RESULTS

Analysis of N. gonorrheae PG. The PG from *N. gonorrheae* strains FA1090 and 1291 was isolated and purified. The general appearance and handling properties of the PG from strain 1291 were typical of those from other bacteria in that it had to be sonicated into suspension. In contrast, the PG from strain FA1090, the genetic source of *N. gonorrheae* Ape1a used in this study, was different as its suspension required only vortexing, and it had a whiter appearance. This white appearance was reflected in the appearance of the originating colonies on the plates. A decrease in the white appearance of the PG could be accomplished with multiple and prolonged Pronase digestions, but it could not be removed completely by this process. Amino acid analysis of hydrolyzed samples of the purified PG from FA1090 confirmed the presence of elevated levels of protein which we presume to be opacity-associated (Opa) proteins characteristic of this and other *N. gonorrheae* strains (*24*).

The percentage of PG O-acetylation for both of these *N. gonorrheae* strains was determined by comparing the amount of base-liberated acetate from isolated and purified samples to their muramic acid contents. This method of data analysis is not affected by the presence of contaminating protein in the different PG samples. The O-acetylation values for strains FA1090 and 1291 (56 ± 3.0 and 50 ± 1.8%, respectively) were similar to previously reported values for other *N. gonorrheae* strains (*25*, *26*). Hence, it appears that the presence of increased protein levels associated with the PG of strain FA1090 does not affect its levels of O-acetylation.

Purification and Activity of Ape1a. The recombinant form of the more soluble, truncated derivative of *N. gonorrheae* Ape1a was purified to >95% homogeneity from the cell lysates of *E. coli* transformants by a combination of affinity and cation-exchange chromatographies. Yields and the levels of purification achieved (Table 1) were similar to those reported previously (*4*). Likewise, the specific activity (Table 1) and Michaelis−Menten parameters (Table 2) obtained with these enzyme preparations using *p*NP-acetate as the substrate were identical to those documented earlier, recognizing the slightly different conditions employed between the studies.

Table 3: Specific Activity of Ape1a and Its Mutant Derivatives on *N. gonorrheae O*-AcetylPG

source strain of *O*-acetylPG	enzyme	specific activity[a] (μmol min^{-1} mg^{-1})
FA1090	Ape1a	0.0492 ± 0.014 (3.8%)
1291	Ape1a	1.29 ± 0.038 (100%)
1291	Asp366 → Ala Ape1a	0.332 ± 0.043 (26%)
1291	His369 → Ala Ape1a	0.0547 ± 0.0011 (4.2%)
1291	Ser80 → Ala Ape1a	≤0.001 (≤0.08%)
1291	Ser152 → Ala Ape1a	1.21 ± 0.031 (94%)
1291	Ser308 → Ala Ape1a	1.29 ± 0.059 (100%)

[a] Reactions were conducted (in at least duplicate) in 50 mM sodium phosphate buffer at pH 7.0 and 37 °C with 5 mg/mL substrate. Percentages in parentheses were calculated relative to Ape1a activity on *O*-acetylPG from strain 1291.

The specific activity of Ape1a was determined using *O*-acetylPG from two *N. gonorrheae* strains as a substrate in sodium phosphate buffer (pH 7.0) containing 0.1% Triton detergent, which was added to aid in the dispersal of the insoluble substrate (Table 3). The activity of Ape1a on *O*-acetylPG from *N. gonorrheae* strain 1291 was very similar to that previously reported using *O*-acetylPG from *Providencia stuartii* (1.29 ± 0.38 μmol min^{-1} mg^{-1} compared to 1.63 ± 0.61 μmol min^{-1} mg^{-1}) (*4*). However, the specific activity of Ape1a on the *O*-acetylPG from *N. gonorrheae* FA1090 was less than 4% of that on strain 1291. This finding was unexpected given that Ape1a was originally cloned from the FA1090 genome, but it presumably reflects the presence of extra protein associated with the PG from FA1090 (described above) which would hinder Ape1a activity. Regardless of the reason, the PG from strain 1291 was used for the remainder of the studies on Ape1a and its mutant derivatives (described below).

Dependence of Ape1a on pH. The substrate *p*NP-acetate was used to determine the effect of pH on the catalytic activity of Ape1a. The assay initially used for this process involved the continuous monitoring of *p*-nitrophenol production at the different pH values that were tested. However, this proved to be troublesome at low pH values as attempts to correct the absorbance extinction coefficients at the different pH values used resulted in unacceptable margins of error. For this reason, we used a discontinuous method to assay Ape1a at various pH values before adjusting the pH to 7 to measure *p*-nitrophenol concentrations. This method proved to be significantly more reliable, but confirmation was obtained periodically by HPLC analysis of reaction mixtures for acetate content.

The Michaelis−Menten parameters for the Ape1a-catalyzed hydrolysis of *p*NP-Ac were determined at different pH values ranging from 3 to 8. The pH−rate plots prepared from these data were sigmoidal (Figure 2), indicating the dependency of the reaction on the ionization of one group. The plot of VE_t^{-1} versus pH provided a pK_{es} value of 6.38 ± 0.24 for the essential ionizable group in the enzyme−substrate complex, while a value of 6.78 ± 0.23 was obtained from the $VE_t^{-1}K_M^{-1}$ versus pH plot for pK_e of a group on the free enzyme. On the basis of these pK_a values, the identity of this ionizable group is likely the imidazolium of a histidyl residue. Using this substrate, values of K_M were found to be independent of pH (data not shown).

Inhibition Studies on Ape1a. To determine if Ape1a functions as a metalloenzyme, like PG *N*-acetylmuramic acid deacetylase (*7*) and PG *N*-acetylglucosamine acetylesterase (*8*), inhibition experiments were conducted with the metal chelator EDTA. As indicated in Table 4, incubation of this reagent at concentrations as high as 10 mM for 30 min prior to assaying resulted in an only minimal loss of activity. Likewise, supplementing reaction mixtures with various cations did not greatly enhance the activity of the enzyme. In fact, rather than stimulating activity, the presence of Zn^{2+}, the cation at the active center of the deacetylases listed above, caused a significant inhibition of Ape1a. These data thus suggested that Ape1a is not a metalloenzyme. In contrast, incubation of Ape1a with the sulfonyl fluorides MSF and PMSF, inhibitors of serine protease/esterases, resulted in the diminution of enzymatic activity. Incubation of the enzyme with increasing concentrations of PMSF and MSF for 30 min provided IC_{50} values for inactivation of 1.7 ± 0.02 and 4.8 ± 0.05 mM, respectively.

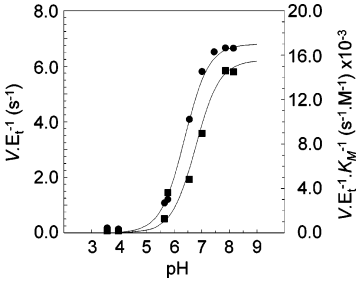

FIGURE 2: Dependence of Ape1a kinetic parameters on pH. The Michaelis−Menten parameters VE_t^{-1} (●) and $VE_t^{-1}K_M^{-1}$ (■) for the Ape1a-catalyzed hydrolysis of *p*NP-acetate were determined in 25 mM sodium acetate buffer (pH 3−6) and 25 mM sodium phosphate buffer (pH 5.5−8). The lines denote the theoretical curves calculated using pK_a values of 6.38 and 6.78, respectively.

Table 4: Effect of Reagents and Cations on Ape1a Activity[a]

reagent or cation	concentration (mM)	residual activity (%)
PMSF	5	2.9
	1	59.1
MSF	5	54.2
EDTA	10	94.2
	1	97.0
Mn^{2+}	1	66.8
Mg^{2+}	1	99.4
Ca^{2+}	1	116
Zn^{2+}	1	21.5

[a] Reactions were conducted (in triplicate) in 50 mM sodium phosphate buffer at pH 6.5 and 20 °C following incubation with an effector for 30 min at 30 °C.

Identification of Potential Catalytic Site Residues for Ape1a. As the inhibition experiments described above suggested Ape1a functions as a serine esterase, a search for potential catalytic Ser, His, and Asp residues within the Ape1a family and related CAZy family CE-3 esterases was conducted. An amino acid sequence alignment of the hypothetical sequences revealed the existence of a number of totally invariant residues (Figure 3). Among these, Ser80 (*N. gonorrheae* Ape1a numbering) of N-terminal signature motif I of the Ape1 enzymes (*3*) and both Asp366 and His369 of C-terminal signature motif VII were identified as possible candidates. Ser152 and Ser308 of the Ape1a enzymes were likewise identified as potential catalytic residues.

In the absence of a known three-dimensional structure of any family CE-3 acetylesterase, the Phyre and 3D-PSSM

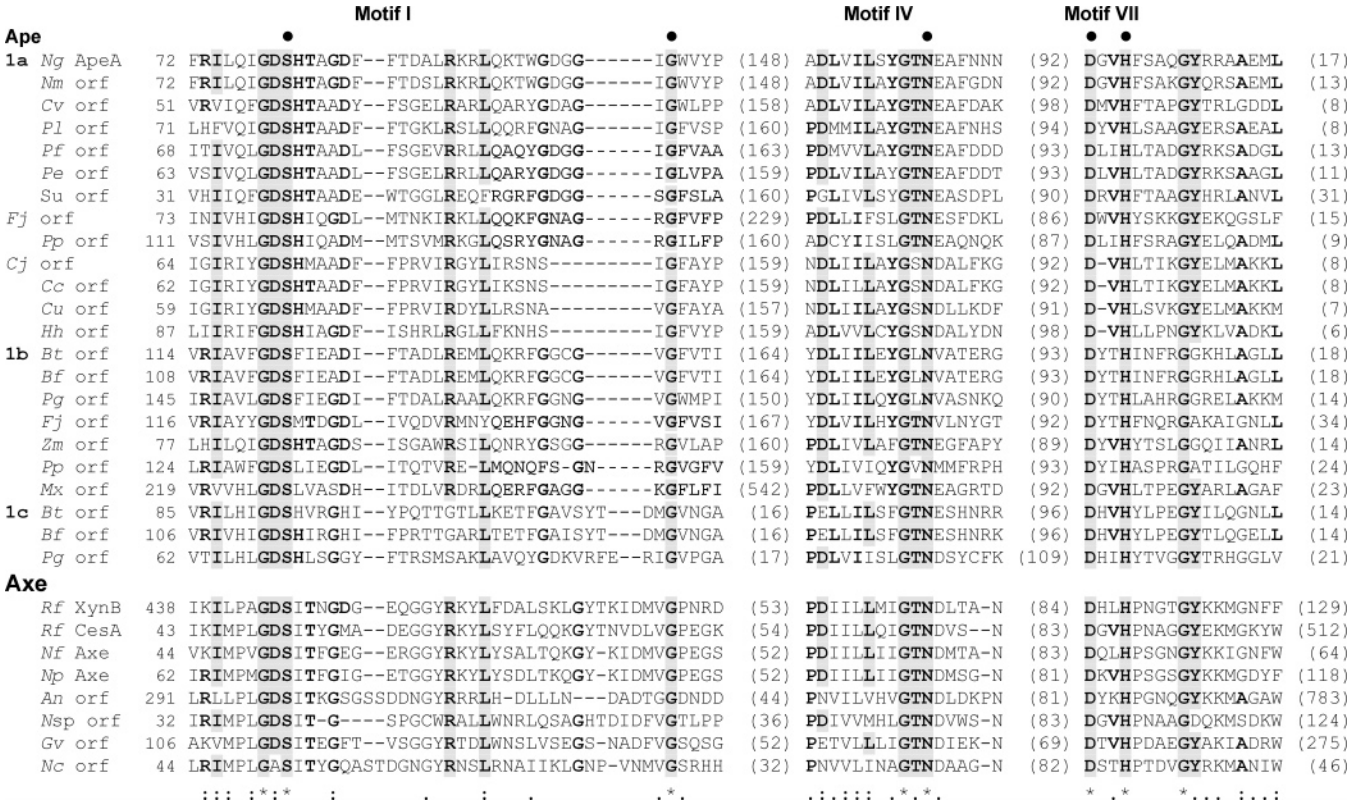

FIGURE 3: Sequence alignment of family CE-3 acetylesterases involving both *O*-acetylPG esterases and acetyl xylan esterases. Depicted in this partial alignment are motifs I, IV, and VII of the seven total consensus motifs in the family 1 *O*-acetylPG esterases (Ape) (*3*) and CE family 3 acetyl xylan esterases (Axe). Boldface residues highlighted in gray denote at least 50 and 80% identity among all sequences, while the filled circles identify residues proposed to comprise the catalytic center and oxyanion hole. The numbers in parentheses denote the number of amino acids linking the presented consensus motifs. Abbreviations (accession numbers) follow. Ape: *Ng*, *N. gonorrheae* (YP_207682); *Nm*, *N. meningitidis* (NP_284202); *Cv*, *Chromobacterium violaceum* (NP_903734); *Pl*, *Photorabdus luminescens* (NP_927853); *Pf*, *Pseudomonas fluorescens* (YP_262936); *Pe*, *Pseudomonas entomophila* (YP_606363); *Su*, *Solibacter usitatus* (ZP_00521423); *Fj*, *Flavobacterium johnsoniae* (1a, ZP_01245343; 1b, ZP_01245344); *Pp*, *Pelodictyon phaeoclathratiforme* (1a, ZP_00588219; 1b, ZP_00588221); *Cj*, *C. jejuni* (NP_281792); *Cc*, *Campylobacter coli* (ZP_00366778); *Cu*, *Campylobacter upsaliensis* (ZP_00369960); *Hh*, *Helicobacter hepaticus* (NP_860613); *Bt*, *Bacteroides thetaiotaomicron* (1b, NP_811595; 1c, NP_811594); *Bf*, *Bacteroides fragilis* (1b, YP_101414; 1c, YP_101413); *Pg*, *Porphyromonas gingivalis* (1b, NP_905385; 1c, NP_905384); *Zm*, *Zymomonas mobilis* (YP_162180); *Mx*, *Myxococcus xanthus* (YP_634625). Axe: *Rf*, *Ruminococcus flavefaciens* (XynB, Q52753; CesA, Q9RLB8); *Nf*, *Neocallimastix frontalis* (AF531435); *Np*, *Neisseria patriciarum* (U66253); *An*, *Aspergillus nidulans* (EAA66937); *N*sp, *Nomomuraea* species (Q7WZ50); *Gv*, *Gloeobacter violaceus* (Q7NGX3); *Nc*, *Neurospora crassa* (XM_323878).

algorithms selected the structure of the GDSL enzyme rhamnogalacturonan acetylesterase from *Aspergillus aculeatus* (PDB entry 1DEO) as the best fit. A fidelity score (*E* value) of 3.0 e^{-15} was obtained using Phyre, and the results predicted that the carboxylic acid side chain of Asp366 and the imidazole side chain of His369 are appropriately positioned to form a salt bridge within a cleft in the enzyme. Unfortunately, the positions of Ser80 and Ser152 could not be located from this prediction because only the core of the Ape1a sequence provided an appropriate fit using the algorithm, and consequently, the N-terminal segment involving residues Met1−Val196 was ignored in the model. However, Ser308 was visualized in the model, and its position was in the proximity of Asp366 and His369.

Purification of Site-Directed Mutants. With the identification of three residues comprising the potential catalytic triad, site-directed mutagenesis was employed to replace each with an Ala residue. All five mutant genes encoding the Ser80 → Ala, Ser152 → Ala, Ser308 → Ala, His369 → Ala, and Asp366 → Ala derivatives of Ape1a were overexpressed in respective *E. coli* transformants as confirmed by SDS−PAGE and Western blot analysis with an anti-His_6 antibody (data not shown). Each mutant enzyme was purified by the same method employed for Ape1a which involves a combination of affinity chromatography on Ni^{2+}NTA-agarose and cation-exchange chromatography on MonoS (*4*). Precaution was taken to ensure that unused (new) chromatography media were employed for these purifications to preclude any potential contamination of the enzyme derivatives with each other. While this protocol served to provide the enzymes in an apparent homogeneous form (data not shown), the recombinant derivatives were obtained in lower yields than Ape1a. As seen in Table 3, the yields for the Ser80 → Ala, His369 → Ala, and Asp366 → Ala mutant proteins were at least 3.5-fold lower than that of Ape1a. Nonetheless, in all cases, sufficient concentrations of homogeneous protein were obtained to permit further characterization of their structure and enzymatic properties.

Determination of the Structure of Mutant Enzymes. Circular dichroism (CD) spectrometry was employed to gain some insight, albeit limited, into the folded state of the mutant Ape1a enzymes. The CD spectra (Figure 5) were analyzed with the algorithm on the Dichroweb server which reported that the secondary structural elements of the His369 → Ala, Ser80 → Ala, Ser152 → Ala, and Ser308 → Ala Ape1a derivatives closely resembled that of wild-type Ape1a

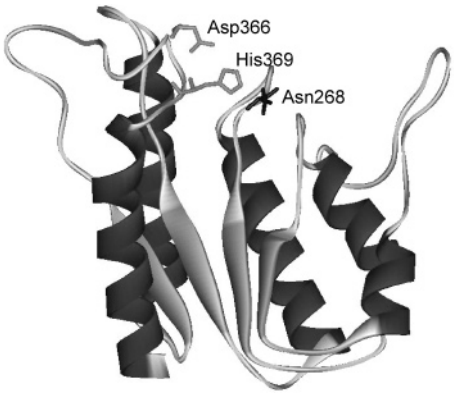

FIGURE 4: Modeled three-dimensional structure of Ape1a. The structure of Apela was modeled on *Aspergillus aculeatus* rhamnogalacturonan acetylesterase (PDB entry 1DEO) using 3D-PSSM. The potential catalytic residues Asp366 and His369 and a component of the oxyanion hole, Asn268, are depicted.

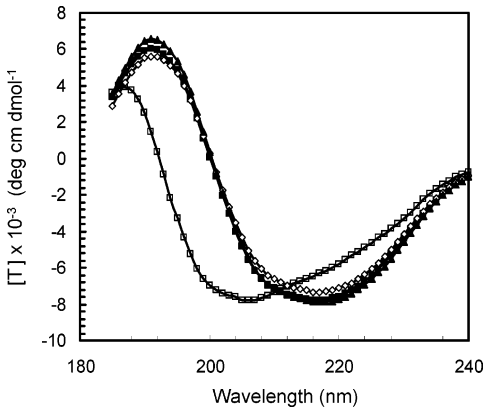

FIGURE 5: Circular dichroism spectra of Ape1a and its mutant derivatives. Spectra of 2.4 μM proteins in 10 mM sodium phosphate buffer at pH 7.0 and 25 °C were recorded in a 0.1 cm path length cell with a scan speed of 50 nm/min. The spectra represent an average of four accumulations: (■) Ape1a, (□) Asp366 → Ala Ape1a, (▲) His369 → Ala Ape1a, and (◇) Ser80 → Ala Ape1a. Data for the Ser152 → Ala and Ser308 → Ala derivatives were identical to those of wild-type Ape1a (not shown).

(Table 5). However, the Asp366 → Ala mutant enzyme appeared to be slightly altered with both the β-strand and helix content lower than those of the wild-type enzyme. This apparent change was unexpected because examination of the amino acid sequence of Asp366 → Ala Ape1a using the Jpred algorithm did not predict any secondary structural alterations.

Enzymatic Properties of Ape1a and Its Mutant Derivatives. The specific activities of the five Ape1a mutant derivatives using the PG from *N. gonorrheae* 1291 as a substrate are presented in Table 3. These data indicate an increasing loss of activity with the replacement of the residues with Ala in the following order: Asp366, His369, and Ser80. In fact, the activity of Ser80 → Ala Ape1a on the insoluble PG substrate was too low to be detected with any accuracy using this assay. On the other hand, the specific activity of the Ser152 → Ala and Ser308 → Ala derivatives was very similar to that of wild-type Ape1a, indicating that these two residues likely do not participate directly in the mechanism of action of the enzyme. For convenience, the Michaelis−Menten parameters of Ape1a and the three affected mutant derivatives were determined for *p*NP-acetate as a substrate. As seen in Table 2, there is little difference in the values of the Michaelis constant K_M of these enzymes. In contrast, large differences in the catalytic constants of the enzymes (V/E_t) were found which, not unexpectedly, followed the same trend that was observed with the specific activity measurements. These changes in turnover number are reflected in the overall catalytic efficiency ($VE_t^{-1}K_M^{-1}$) of the enzymes such that the Ser80 → Ala mutant was at least 5 orders of magnitude less efficient than the wild-type enzyme. It should be noted, however, that the observed activity of the Ser80 → Ala derivative was at the level of detection limits, and despite attempts to account for the spontaneous hydrolysis of the substrate, the Michaelis−Menten parameters calculated for this enzyme are likely misleading. This view is consistent with the level of experimental error associated with these data.

DISCUSSION

We recently reported Ape1a as the first esterase to be identified with activity on O-acetylated PG (*4*). On the basis of its amino acid sequence, this enzyme was found to be related to family CE-3 of carbohydrate estereases that is comprised of acetyl xylan esterases (*3*). Despite the increasing number of characterized and hypothetical enzymes belonging to the CE-3 family, nothing was previously known about their mechanism of action. In this study, we have provided several lines of evidence to indicate that Ape1a, and possibly the CE-3 enzymes too, functions as a serine esterase. (i) The activity of the enzyme is dependent upon a charged amino acid residue with pK_a values for the free enzyme and enzyme−substrate complex consistent with those of histidine. (ii) Sulfonyl fluorides, but not metal chelator, inhibit activity. (iii) Metal ions either had no effect or inhibit catalytic activity. (iv) Replacement of the Ser, His, and Asp residues invariant in all of the aligned sequences is important for turnover but not substrate binding. (v) The relative importance of these residues increases from Asp366 to His369 and then Ser80. This trend of the loss of activity in the respective site-directed mutants is consistent with Ser80 playing the most important role in a catalytic triad involving His369 and Asp366 in a manner analogous to the classic mechanistic action of the serine protease/esterase/lipase superfamily of enzymes. Thus, we propose that a salt bridge exists between the carboxyl group of Asp366 and the imidazolium side chain of His369 in the active state of Ape1a (and presumably the CE-3 enzymes). This salt bridge would permit the imidazolium group to participate in a proton relay to abstract a proton from its neighboring Ser80 residue, rendering the latter nucleophilic and suitable to function as a catalytic residue (Figure 6). This Ser nucleophile would attack the carbonyl carbon of an ester-linked acetate group on the substrate (**1**), leading to the formation of a tetrahedral transition state (**2**) which would subsequently collapse to a covalent acyl−enzyme intermediate (**3**) and the associated release of the PG product. The acetate would then be hydrolyzed from Ser80 (i.e., deacylation) in a reversal of this process (**4**) with water playing the role of the departed C-6 hydroxyl group of the muramoyl residue, thereby returning Ser80 to its protonated state and making it ready for another catalytic event.

If the mechanism described above does indeed apply to Apela, then the transient negatively charged oxygen atom associated with the transition state would have to be

Table 5: Secondary Structure of Ape1a and Its Derivatives[a]

	helix 1	helix 2	strand 1	strand 2	turns	unordered	total
Ape1a	0.08	0.1	0.172	0.103	0.209	0.39	1.049
Asp366 → Ala Ape1a	0.07	0.07	0.141	0.095	0.215	0.408	0.999
His369 → Ala Ape1a	0.09	0.1	0.172	0.101	0.201	0.376	1.033
Ser80 → Ala Ape1a	0.08	0.09	0.172	0.103	0.2	0.366	1.004

[a] The CD data presented in Figure 4 were analyzed using Selecon 3 with protein reference set 3 (Dichroweb Server) and are presented as an average of four accumulations.

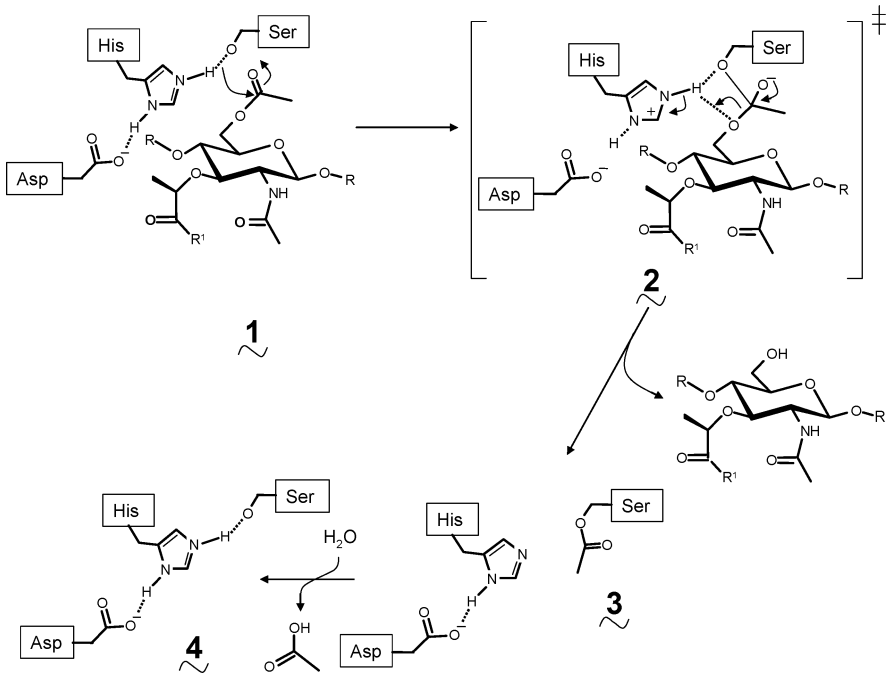

FIGURE 6: Proposed mechanism of action of Ape1a and family CE-3 acetylesterases. R and R′ denote β-1,4-linked GlcNAc residues and stem peptides, respectively.

stabilized by hydrogen bonds to appropriately positioned residues forming an "oxyanion hole". The identity of these latter residues has yet to be determined, and knowledge of the three-dimensional structure of Ape1a, or for that matter any CE-3 enzyme, would be helpful. In this regard, we have attempted to obtain appropriate crystals of Ape1a for structural analysis, but unfortunately, the best resolution achieved to date is only 3.2 Å (A. Matte and R. Shi, personal communication). Nonetheless, a closer inspection of the aligned amino acid sequences of the CE-3 enzymes suggests that they may represent SGNH hydrolases. The SGNH hydrolases are a subfamily of the GDSL esterases that have recently been identified on the basis of the discovery of four invariant residues found in separate conserved blocks throughout the member proteins (*27*). The catalytic Ser in block I, the amide of the Gly residue in block II, and the $N^{\delta 2}$ atom of the Asn residue in block III each participate as proton donors in the formation of the oxyanion hole, while the His participates as the base in the catalytic triad. With Ape1a, the respective invariant residues would correspond to Gly125 of consensus motif I (*3*) and Asn268 of motif IV, in addition to the catalytic Ser80 and His369 residues (Figure 3). Unfortunately, again for the reasons stated above, only Asn268 can be visualized in the modeled three-dimensional structure of Ape1a, but indeed, its $N^{\delta 2}$ proton would be positioned appropriately to comprise the oxyanion hole in the active site cleft (Figure 4). In the absence of a known structure, we have initiated genetic engineering experiments to confirm the assignment of these residues as comprising the oxyanion hole.

Although there was a dearth of information pertaining to the mechanism of action of the CE-3 enzymes, structural information for the acetyl xylan esterases belonging to families CE-4, CE-5, CE-6, and CE-7 has been obtained and has provided insight into their mechanisms. Whereas the deacetylases of family CE-4 have been shown to be metalloenzymes (*7*−*11*), the enzymes of the other three families are reported to function as serine esterases. These conclusions have been largely based on structural considerations as mechanistic studies have been performed with only the CE-7 acetyl xylan esterases from *Bacillus pumilus* (*28*) and *B. subtilis* (*29*). These latter investigations involved the site-specific replacement of the putative catalytic Ser residues with Ala. However, while stating that the mutant enzymes were inactive, neither study presented kinetic details. Nonetheless, the three-dimensional structures of each of these CE-5 (*30*−*32*), CE-6 (PDB entry 1ZMB), and CE-7 (*29*; PDB entry 1VLQ) enzymes do appear to have active sites comprised of Ser, His, and Asp residues positioned appropriately to form a catalytic triad.

The active site environment of the GDSL serine proteases/esterases has been found to be highly flexible, and relatively large conformational changes occur upon substrate binding (reviewed in ref *27*). This observation led to the suggestion that the flexibility may facilitate binding to a wide range of substrates and confer versatile functional properties (*33*). It

remains to be determined if such flexibility exists in the active site pocket of Ape1a, but such would explain its ability to utilize both acetyl xylan and *O*-acetylPG as substrates. Presumably, the more simple xylan homopolymer can be accommodated in the active site cleft that otherwise preferentially binds to the complex heteropolymer PG. A flexible active site might also account for the relatively poor inhibition we observed with the sulfonyl fluorides. The modification of the nucleophilic Ser residue in the Ser proteases/esterases usually requires concentrations of the reagents of no more than 1 mM to achieve absolute inhibition within a matter of minutes (*34*). However, as with a number of other related GDSL esterases, including the CE-5 acetyl xylan esterase from *Hypocrea jecorina* (formerly *Trichoderma reesei*), elevated concentrations of the sulfonyl fluorides for prolonged exposure times were required to achieve complete inhibition of Ape1a. In the extreme case of LipA, a lipase from a *Ralstonia* sp., 57% of the enzyme activity remained following treatment with 10 mM PMSF (*35*). While steric hindrance was found to preclude accessibility of the reagent to the catalytic Ser of palmitoyl-protein thioesterase (*36*), it is possible that in the resting state of a number of the other "resistant" serine esterases, the reagents remain relatively inaccessible to the active site in a "closed" conformation.

As noted earlier, the catalytic power of Ape1a was found to be 10^8 when its k_{cat} for *p*-NP-acetate was compared with the pseudo-first-order rate constant for the spontaneous hydrolysis of this synthetic substrate at the same temperature and pH. Although this catalytic power is similar to that of some xylan acetylesterases, it is considerably lower than that associated with other Ser proteases and esterases. For example, values on the order of 10^{10} and 10^{13} have been reported for the Ser protease subtilisin (*37*) and acetylcholine esterase (*38*), respectively, both of which catalyze the deacylation of an acyl−Ser intermediate. One possible explanation for this apparent reduced catalytic power could concern the nature of the in vitro assay conditions employed for the study of the enzyme. Ape1a is thought to be a peripheral membrane enzyme, associated with the inner leaflet of the outer membrane of Gram-negative bacteria, and functions on a totally insoluble substrate, PG. Clearly, the assay conditions employed in vitro do not mimic this environment very well. Moreover, it is conceivable that the in vivo conditions induce a more catalytically favorable conformation of the enzyme. That different conformational forms of Ape1a exist is suggested by our inability to obtain high-resolution structural information with crystals of the enzyme due to an apparent mosaicity of the crystals (A. Matte and R. Shi, personal communication).

Previously, the activity of Ape1a was tested on *O*-acetylPG from *P. stuartii* and not on PG from the enzyme's native background, *N. gonorrheae* (*4*). To do this, the PG from *N. gonorrheae* strains 1291 and FA1090 first had to be characterized for their O-acetyl content as this was previously unknown despite the fact that a number of other strains have been examined (reviewed in refs *1* and *2*). Quantitative analysis indicated that these PGs were O-acetylated to nearly the same extent, but the ability of Ape1a to utilize them as a substrate was found to differ significantly. Further analysis of the respective PGs revealed the presence of associated protein(s), with the more recalcitrant PG from strain FA1090. Presumably, these cell wall-associated proteins are Opa proteins characteristic of some Neisserial strains (*24*); FA1090 is reported to have 11 distinct Opa proteins (*39*). The apparent inhibition caused by the presence of these Opa proteins suggests that, as with the activity of the lytic transglycosylases and possibly other autolysins being inhibited by the presence of O-acetyl groups on PG (*40*, *41*), the *O*-acetylPG esterases are likewise inhibited by the presence of these PG-associated proteins. This would imply that, for the normal metabolism of PG in these strains, one or more proteases would be required to provide appropriate access at specific sites for PG biosynthesis and turnover, which could thus provide yet another level of control for these processes.

As noted above, autolytic activity, especially that of the lytic transglycosylases, has been shown to be regulated by the presence of O-acetyl groups on the C-6 position of muramoyl residues in PG (*40*, *41*). Indeed, the lytic transglycosylases strictly require a free hydroxyl group at this C-6 position for their activity to form the 1,6-anhydromuramoyl product. As Ape1a appears to be responsible for the removal and/or remodeling of O-acetyl groups on PG, it must play an at least indirect role in this regulation. The knowledge gained in this study of the mechanism of action of *O*-acetylPG esterases may prove to be very useful in the design of specific inhibitors which could lead to the development of a novel class of antibacterial compounds that target bacteria that produce O-acetylated PG. Among these are many important human pathogens, including *Neisseria menningitidis*, *Staphylococcus aureus* (*1*, *2*), as well as species of *Campylobacter*, *Helicobacter*, and *B. anthracis* (*3*), in addition to *N. gonorrheae.*

ACKNOWLEDGMENT

We thank Chris Vandenende and Chelsea A. Clarke for expert technical assistance.

SUPPORTING INFORMATION AVAILABLE

Tables listing the bacterial strains and plasmids used in this study and the sequences of the oligonucleotides used for site-directed mutagenesis of *ape1a*. This material is available free of charge via the Internet at http://pubs.acs.org.

REFERENCES

1. Clarke, A. J., Strating, H., and Blackburn, N. T. (2000) Pathways for the *O*-acetylation of bacterial cell wall polysaccharides, in *Glycomicrobiology* (Doyle, R. J., Ed.) pp 187−223, Plenum Publishing Co. Ltd., New York.
2. Clarke, A. J., and Dupont, C. (1992) *O*-Acetylated peptidoglycan: Its occurrence, pathobiological significance, and biosynthesis, *Can. J. Microbiol. 38*, 85−91.
3. Weadge, J. T., Pfeffer, J. M., and Clarke, A. J. (2005) Identification of a new family of enzymes with potential *O*-acetylpeptidoglycan esterase activity in both Gram-positive and Gram-negative bacteria, *BMC Microbiol. 5*, 49.
4. Weadge, J. T., and Clarke, A. J. (2006) Identification and characterization of *O*-acetylpeptidoglycan esterase: A novel enzyme discovered in *Neisseria gonorrhoeae*, *Biochemistry 45*, 839−851.
5. Caufrier, F., Martinou, A., Dupont, C., and Bouriotis, V. (2003) Carbohydrate esterase family 4 enzymes: Substrate specificity, *Carbohydr. Res. 338*, 687−692.
6. Dupont, C., Daigneault, N., Shareck, F., Morosoli, R., and Kluepfel, D. (1996) Purification and characterization of an acetyl

xylan esterase produced by *Streptomyces lividans*, *Biochem. J. 319*, 881−886.
7. Blair, D. E., and van Aalten, D. M. (2004) Structures of *Bacillus subtilis* PdaA, a family 4 carbohydrate esterase, and a complex with *N*-acetyl-glucosamine, *FEBS Lett. 570*, 13−19.
8. Blair, D. E., Schuttelkopf, A. W., MacRae, J. I., and van Aalten, D. M. (2005) Structure and metal-dependent mechanism of peptidoglycan deacetylase, a streptococcal virulence factor, *Proc. Natl. Acad. Sci. U.S.A. 102*, 15429−15434.
9. Taylor, E. J., Gloster, T. M., Turkenburg, J. P., Vincent, F., Brzozowski, A. M., Dupont, C., Shareck, F., Centeno, M. S., Prates, J. A., Puchart, V., Ferreira, L. M., Fonts, C. M., Biely, P., and Davies, G. J. (2006) Structure and activity of two metal ion-dependent acetylxylan esterases involved in plant cell wall degradation reveals a close similarity to peptidoglycan deacetylases, *J. Biol. Chem. 281*, 10968−10975.
10. Puchart, V., Gariépy, M., Shareck, F., and Dupont, C. (2005) Identification of catalytically important amino acid residues of *Streptomyyces lividans* acetylxylan esterase A from carbohydrate esterase family 4, *Biochim. Biophys. Acta 1764*, 263−274.
11. Blair, D. E., Hekmat, O., Schuttelkopf, A. W., Shrestha, B., Tokuyasu, K., Withers, S. G., and van Aalten, D. M. (2006) Structure and mechanism of chitin deacetylase from the fungal pathogen *Colletotrichum lindemuthianum*, *Biochemistry 45*, 9416−9426.
12. Davies, G. J., Gloster, T. M., and Henrissat, B. (2005) Recent structural insights into the expanding world of carbohydrate-active enzymes, *Curr. Opin. Struct. Biol. 15*, 637−645.
13. Kellogg, D. S., Jr., Peacock, J. R., Deacon, W. F., Brown, L., and Pirkle, C. I. (1963) *Neisseria gonorrhoeae*. I. Virulence genetically linked to clonal variation, *J. Bacteriol. 85*, 1274−1279.
14. Pagotto, F., Salimnia, H., Totten, P. A., and Dillon, J. R. (2000) Stable shuttle vectors for *Neisseria gonorrhoeae*, *Haemophilus* spp. and other bacteria based on a single origin of replication, *Gene 244*, 13−19.
15. Dupont, C., and Clarke, A. J. (1991) Dependence of lysozyme-catalysed solubilization of *Proteus mirabilis* peptidoglycan on the extent of *O*-acetylation, *Eur. J. Biochem. 195*, 763−769.
16. Clarke, A. J. (1993) Compositional analysis of peptidoglycan by high performance anion-exchange chromatography, *Anal. Biochem. 212*, 344−350.
17. Clarke, A. J. (1993) Extent of peptidoglycan *O*-acetylation in the tribe *Proteeae*, *J. Bacteriol. 175*, 4550−4553.
18. Sreerama, N., and Woody, R. W. (2000) Estimation of protein secondary structure from CD spectra: Comparison of CONTIN, SELCON and CDSSTR methods with an expanded reference set, *Anal. Biochem. 287*, 252−260.
19. Sreerama, N., Venyaminov, S. Y., and Woody, R. W. (2000) Estimation of protein secondary structure from CD spectra: Inclusion of denatured proteins with native protein in the analysis, *Anal. Biochem. 287*, 243−251.
20. Laemmli, U. K. (1970) Cleavage of structural proteins during the assembly of the head of bacteriophage T4, *Nature 227*, 680−685.
21. Kelley, L. A., MacCallum, R. M., and Sternberg, M. J. E. (2000) Enhanced genome annotation using structural profiles in the program 3D-PSSM, *J. Mol. Biol. 299*, 499−520.
22. Fischer, D., Barret, C., Bryson, K., Elofsson, A., Godzik, A., Jones, D., Karplus, K. J., Kelley, L. A., Maccallum, R. M., Pawowski, K., Rost, B., Rychlewski, L., and Sternberg, M. J. (1999) CAFASP-1: Critical assessment of fully automated structure prediction methods, *Proteins: Struct., Funct., Genet. Suppl. 3*, 209−217.
23. Kelley, L. A., Maccallum, R., and Sternberg, M. J. E. (1999) *Proceedings of the Third Annual Conference on Computational Molecular Biology*, pp 218−225, The Association for Computing Machinery, New York.
24. Hauck, C. R., and Meyer, T. F. (2003) "Small" talk: Opa proteins as mediators of *Neisseria*-host-cell communication, *Curr. Opin. Microbiol. 6*, 43−49.
25. Swim, S. G., Gfell, M. A., Wilde, C. E., III, and Rosenthal, R. S. (1983) Strain distribution in extents of lysozyme resistance and *O*-acetylation of gonococcal peptidoglycan determined by high-performance liquid chromatography, *Infect. Immun. 42*, 446−452.
26. Rosenthal, R. S., Blundell, J. K., and Perkins, H. R. (1982) Strain-related differences in lysozyme sensitivity and extent of O-acetylation of gonococcal peptidoglycan, *Infect. Immun. 37*, 826−829.
27. Akoh, C. C., Lee, G., Liaw, Y., Huang, T., and Shaw, J. (2004) GDSL family of serine esterases/lipases, *Prog. Lipid Res. 43*, 534−552.
28. Krastanova, I., Guarnaccia, C., Zahariev, S., Degrassi, G., and Lamba, D. (2005) Heterologous expression, purification, crystallization, X-ray analysis and phasing of the acetyl xylan esterase from *Bacillus pumilus*, *Biochim. Biophys. Acta 1748*, 222−230.
29. Vincent, F., Charnock, S. J., Verschueren, K. H., Turkenburg, J. P., Schott, D. J., Offen, W. A., Roberts, S., Pell, G., Gilbert, H. J., Davies, G. J., and Brannigan, J. A. (2003) Multifunctional xylooligosaccharide/cephalosporin C deacetylase revealed by the hexameric structure of the Bacillus subtilis enzyme at 1.9 Å resolution, *J. Mol. Biol. 330*, 593−606.
30. Hakulinen, N., Tenkanen, M., and Rouvinen, J. (2000) Three-dimensional structure of the catalytic core of acetylxylan esterase from *Trichoderma reesei*: Insights into the deacetylation mechanism, *J. Struct. Biol. 132*, 180−190.
31. Ghosh, D., Sawicki, M., Lala, P., Erman, M., Pangborn, W., Eyzaguirre, J., Gutierrez, R., Jornvall, H., and Thiel, D. J. (2001) Multiple conformations of catalytic serine and histidine in acetylxylan esterase at 0.90 Å, *J. Biol. Chem. 276*, 11159−11166.
32. Ghosh, D., Erman, M., Sawicki, M., Lala, P., Weeks, D. R., Li, N., Pangborn, W., Thiel, D. J., Jornvall, H., Gutierrez, R., and Eyzaguirre, J. (1999) Determination of a protein structure by iodination: The structure of iodinated acetylxylan esterase, *Acta Crystallogr. D55*, 779−784.
33. Huang, Y. T., Liaw, Y. C., Gorbatyuk, V. Y., and Huang, T. H. (2001) Backbone dynamics of *Escherichia coli* thioesterase/protease I: Evidence of a flexible active-site environment for a serine protease, *J. Mol. Biol. 307*, 1075−1090.
34. Karpushova, A., Brümmer, F., Barth, S., Lange, S., and Schmid, R. D. (2005) Cloning, recombinant expression and biochemical characterization of novel esterases from *Bacillus* sp. associated with the marine sponge *Aplysina aerophoba*, *Appl. Microbiol. Biotechnol. 67*, 59−69.
35. Quyen, D. T., Le, T. T. G., Nguyen, T. T., Oh, T., and Lee, J. (2005) High-level heterologous expression and properties of a novel lipase from *Ralstonia* sp. M1, *Protein Expression Purif. 28*, 102−110.
36. Das, A. K., Bellizzi, J. J., III, Tandel, S., Biehl, E., Clardy, J., and Hofmann, S. L. (2000) Structural basis for the insensitivity of a serine enzyme (palmitoyl-protein thioesterase) to phenylmethylsulfonyl fluoride, *J. Biol. Chem. 275*, 23847−23851.
37. Carter, P., and Wells, J. A. (1988) Dissecting the catalytic triad of a serine protease, *Nature 332*, 564−568.
38. Viragh, C., Harris, T. K., Reddy, P. M., Massiah, M. A., Mildvan, A. S., and Kovach, I. M. (2000) NMR evidence for a short, strong hydrogen bond at the active site of a cholinesterase, *Biochemistry 39*, 16200−16205.
39. Dempsey, J. A., Litaker, W., Madhure, A., Snodgrass, T. L., and Cannon, J. G. (1991) Physical map of the chromosome of *Neisseria gonorrhoeae* FA1090 with locations of genetic markers, including *opa* and *pil* genes, *J. Bacteriol. 173*, 5476−5486.
40. Strating, H., and Clarke, A. J. (2001) Differentiation of bacterial autolysins by zymogram analysis, *Anal. Biochem. 290*, 388−393.
41. Payie, K. G., Strating, H., and Clarke, A. J. (1996) The role of *O*-acetylation in metabolism of peptidoglycan in *Providencia stuartii*, *Microb. Drug Resist. 2*, 135−140.
42. Apicella, M. A. (1974) Antigenically distinct populations of *Neisseria gonorrhoeae:* Isolation and characterization of the responsible determinants, *J. Infect. Dis. 130*, 619−625.

BI700254M